

29.5mA. The IF level at 2GHz measured using a spectrum analyser is shown in Fig. 4 with the levels of LO and RF. These millimetre-signal values were measured at the output of the Gunn oscillator and the tripler. Fig. 5 shows that the down-converted IF signal is flat except at the band edge and the point of 94.3GHz. The signals for LO and RF were weak at the band edge. There is no major frequency-dependent element on the chip; therefore this chip has very high-frequency, wideband characteristics in the millimetre-frequency range. We cannot determine the reason for the degradation of the IF signal at the 94.3GHz LO; it may be due to the spatial resonance of the case. In the measurement of another IC pattern of the HBT amplifier only, the gain was 14dB at 2 GHz and the -3dB bandwidth was 12GHz. This is the upper limitation of the IF signal.

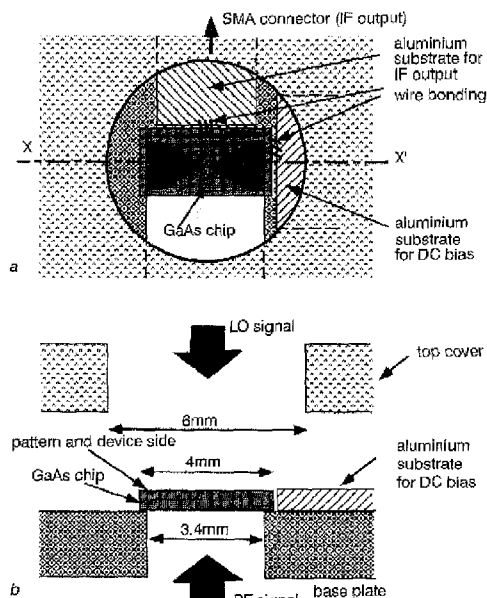


Fig. 3 Schematic diagram of mounting

a Top view  
b Cross-sectional view

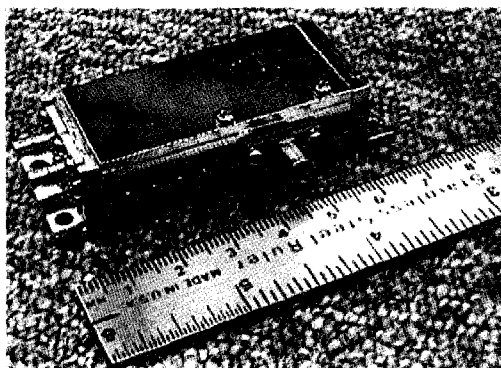


Fig. 4 Photograph of module

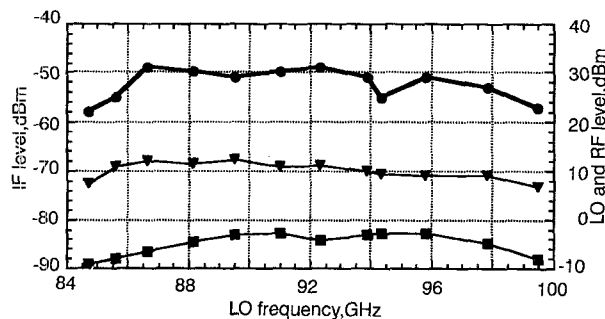


Fig. 5 Frequency characteristics of module

● IF level  
▼ LO level  
■ RF level

As the next step, we should investigate the structure of the case without any resonance in the frequency range of interest, and the antenna pattern of our chip. We have not used any focusing element for the millimetre-wave signals. Lenses might be needed at the top and the bottom of the chip [5].

**Conclusion:** Full monolithic integration of the antenna, the mixer and the amplifier was reported. The characteristics were measured in a millimetre-wave frequency, from 84.7 to 99.5GHz. The integration of these elements is useful because the losses due to the interface between the chip and transmission line can be neglected.

**Acknowledgment:** We would like to thank A. Mase for informative discussions, and H. Nakamura and H. Hosomatsu for their continuous encouragement and guidance.

© IEE 1997

1 September 1997

Electronics Letters Online No: 19971236

H. Matsuura, K. Tezuka, I. Aoki, M. Yamanaka, S. Kobayashi, T. Fujita and A. Miura (Teratec Corporation, 2-9-32 Naka-cho, Musashino, Tokyo 180, Japan)

Y. Nagayama (National Institute for Fusion Science, 322-6 Oroshi-cho, Toki 509-52, Japan)

## References

- 1 AOKI, I., TEZUKA, K., MATSUURA, H., KOBAYASHI, S., FUJITA, T., and MIURA, A.: '80 GHz AlGaAs HBT oscillator'. IEEE 1996 GaAs IC Symp. Dig., 1996, pp. 281-284
- 2 MATSUURA, H., TEZUKA, K., AOKI, I., MIURA, A., YAMANAKA, M., YAKIHARA, T., KOBAYASHI, S., OKA, S., FUJITA, T., and MURATA, D.: 'A monolithic W-band CPW rat-race mixer with HBT IF amplifier'. IEEE 1996 MTT-S Dig., 1996, pp. 389-393
- 3 MATSUURA, H., TEZUKA, K., AOKI, I., YAMANAKA, M., KOBAYASHI, S., FUJITA, T., and MIURA, A.: 'Monolithic rat-race mixers for millimeter waves'. 1997 Topical Symp. Millimeter Waves (TSMW 97) Dig., 1997, pp. 46-47
- 4 ROY, L.: '30GHz GaAs monolithic low noise amplifier-antennas'. IEEE 1997 MTT-S Dig., 1997, pp. 967-970
- 5 KONISHI, Y., KAMEGAWA, M., CASE, M., YU, R., ALLEN, S.T., and RODWELL, M.J.W.: 'A broadband free-space millimeter-wave vector transmission measurement system', IEEE Trans. MTT, 1994, MTT-42, (7), pp. 1131-1139

## Compact artificial neural network approach for multiple fault location in digital circuits

T. Arslan and A. Al-Jumah

Indexing terms: Neural networks, Digital circuits

The authors report a new approach for the diagnosis of multiple faults using artificial neural networks (ANNs). The approach utilises a compact and efficient set of data derived from a set of test patterns generated for a given circuit. It is demonstrated that the approach will lead to a higher multiple faults diagnosis performance, in addition to a significant reduction in the size of the ANN and the training data, hence enabling failure diagnosis of larger and more complex systems.

**Introduction:** A local defect in a VLSI device may cause multiple stuck-at faults instead of single stuck-at faults. With the increase in the complexity of such devices, the probability of multiple faults occurring will increase significantly. Dealing with multiple faults is a complex task because of the large number of combinations of such faults. For example, a circuit with  $N$  nets may have up to  $3^N - 1$  faults. Owing to the large number of multiple faults possible in the circuit, using the single stuck-at fault to detect multiple faults will be easier and more efficient [1]. For this reason there is a demand for effective methods of treating such faults.

Numerous research papers have tackled the issue of multiple faults, however most of these have concentrated on aspects of test pattern generation, as in, for example [2 - 4]. Artificial neural

networks (ANNs) have been used for the diagnosis of multiple faults after being trained with single stuck-at failure information from a fault truth table (FTT) [5]. Such a table usually lists all single-fault/no-fault conditions in the circuit against the resulting state of both internal and external nets. To obtain acceptable diagnosis performance, the ANN needs to be trained with all entries in the FTT [5], which increases exponentially with circuit size. Even then the diagnosis performance is ~81% for single fault detection and 4% for two faults detection.

In this Letter we demonstrate that using an approach based on ANNs trained with test pattern sets generated using an automatic test pattern generation system can lead to a higher multiple fault diagnosis performance and a significant reduction in the size of the ANN and the training data, hence enabling the diagnosis of larger and more complex systems.

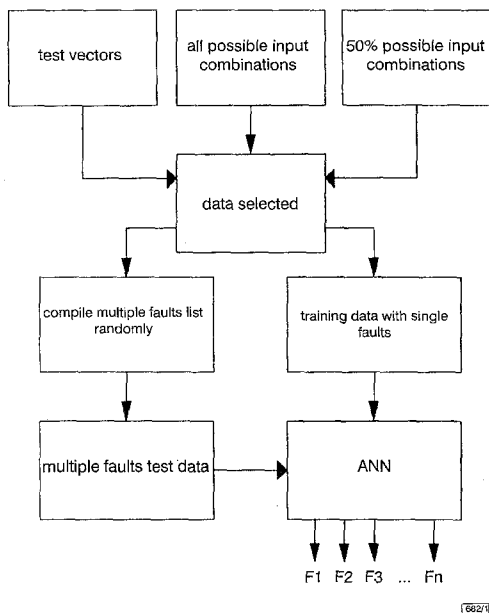


Fig. 1 Flowchart of diagnostic system

**Procedure:** The performance of the ANN is investigated using three different types of randomly selected data. These types are derived from data corresponding to all possible input combinations in the FTT, 50% of possible input combinations in the FTT and the use of test vectors alone. In each case, the ANN is trained with single fault information from the FTT and is tested by its ability to diagnose multiple faults. Fig. 1 illustrates the flowchart of the proposed method.

Table 1: Fault truth table of example circuit

		f-free		i1/0		i2/1		g1/0	
i1	i2	g1	g2	g1	g2	g1	g2	g1	g2
0	0	1	0	1	0	1	0	0	1
0	1	1	0	1	0	1	0	0	1
1	0	1	0	1	0	0	1	0	1
1	1	0	1	1	0	0	1	0	1

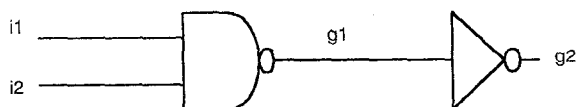


Fig. 2 Example circuit

The training data is formed using a single fault, while the testing data is compiled randomly with multiple faults. The inputs to the ANN are consecutive sets of binary circuit inputs and the corresponding outputs fed in a serial form for each set of input combinations in the FTT. The number of input sets fed into the ANN is dependent on the type of the data selected (all possible input combinations, 50% of possible input combinations or the test

vectors). To illustrate the data representation method adopted, the example in Fig. 2 is used. Table 1 represents the FTT of the circuit when the input i1 is stuck-at 0 (i1/0), input i2 is stuck-at 1 (i2/1) and the output g1 is stuck-at 0 (g1/0).

All combinations of data presented to the ANN for the circuit in Fig. 2 are shown in Table 2. Each entry in the table is formed by sequences of the string i1 i2 g1 g2 repeated for all i1 and i2 combinations in Table 1. This is repeated for each of the cases: fault-free, i1 stuck-at 0 (i1/0), i2 stuck-at 1 (i2/1) and g1 stuck-at 0 (g1/0). Each case (row) represents a separate input pattern to the ANN.

Table 2: ANN inputs

f-free	0	0	1	0	0	1	1	0	1	0	1	1	0	1
i1/0	0	0	1	0	0	1	1	0	0	1	0	0	1	1
i2/1	0	0	1	0	0	1	1	0	1	1	0	1	1	0
g1/0	0	0	0	1	0	1	0	1	1	0	0	1	1	0

The ANN output representation is as follows: a '1' output indicates a fault in a corresponding gate whereas a '0' indicates a fault free gate. In this study 0.1 is used instead of binary '0' and 0.9 instead of binary '1', to overcome the boundary effects of the sigmoid activation function.

Initial investigations showed that an ANN using a multilayer perceptron with backpropagation algorithm is suitable for this work. The ANN consists of three layers. The number of neurons in the input layer is dependent on the type of data selected. In this study when C17 is used, for example, the number of input neurons with all possible input combinations, 50% of possible input combinations and test vectors are 352, 176 and 44, respectively. The number of neurons in the hidden layers is 35 for all cases. The number of neurons in the output layer equals the number of possible single faults in the circuit, which in this case is 23 neurons.

**Results:** Two circuits are used to demonstrate the proposed ANN diagnostic system, the C17 ISCAS benchmark circuit and the circuit, C1 shown in Fig. 3.

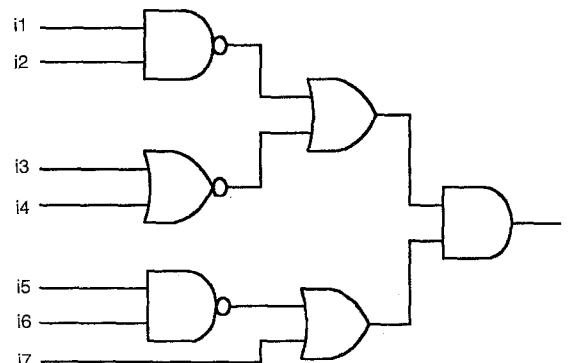


Fig. 3 Example circuit C1

Table 3: Fault diagnosis performance of ANNs in C17

ANN size In:Mid:Out	1 fault detected	2 faults detected	Incorrectly detected
	%	%	
352:35:23	86.98	40.9	1
176:35:23	85.87	20.46	1
44:35:23	100	72	0

Table 3 shows the results when random multiple faults are inserted in the circuit of C17. The results give the diagnostic performance for one fault detection, two faults detection and the number of incorrectly detected faults. Each combination of random faults are tested using the three data selection types mentioned above. For each data selection type, four different examples of test data with randomly selected multiple faults have been chosen. The results in Table 3 represent the average. In the case of single fault detection, the diagnostic performance of the ANN is 86.98% when all possible input combinations are used and 85.87%

when 50% of the possible input combinations are used, whereas the diagnostic performance is increased to 100% when the test vectors are used. For two fault detection, the diagnostic performance of the ANN is 40.9% when all possible input combinations are

**Table 4:** ANN diagnostic performance using test vectors

Fault detection	C1	C17
1 fault detected [%]	100	100
2 faults detected [%]	75	72
Incorrectly detected	0	0

used, 20.46% when 50% of the possible input combinations are used and increases to 72% when the test vectors are used. Table 4 shows the diagnosis performance with one fault and two faults for the circuits C1 and C17. It is clear from the Table that the diagnostic performance for one fault is 100% in both circuits and the diagnostic performance for two faults is 75 and 72% for C1 and C17, respectively. Also, the number of incorrectly detected faults in both circuits is zero. This clearly shows the superiority of using test vectors.

**Conclusion:** The study clearly shows that an ANN can be used successfully in the fault diagnosis of multiple stuck-at faults in digital circuits. Furthermore, using test vectors and an improved method of data representation for the ANN, the fault diagnostic system produces significant improvement in the diagnosis of multiple faults.

© IEE 1997

23 July 1997

*Electronics Letters Online No: 19971211*

T. Arslan and A. Al-Jumah (*Cardiff University of Wales, School of Engineering, Cardiff CF2 3TF, United Kingdom*)

## References

- STEPHEN, S.Y., and SHIH-CHIEN, Y.: 'Multiple fault detection of combinational logic circuits', *IEEE Trans.*, 1975, **C-24**, (3), pp. 233-242
- KUO, T.Y., WANG, J.F., and LEE, J.Y.: 'Multiple fault detection using single-fault tests', *Electron. Lett.*, 1991, **27**, (15), pp. 1329-1330
- WEN-BEN, J., and PATRICK, H.M.: 'Multiple fault testing using minimal single fault test set for fanout-free circuits', *IEEE Trans. Comput.-Aided Des. Integr. Circuits Syst.*, 1993, **12**, (1), pp. 149-157
- LAI, K., and LALA, P.K.: 'Multiple fault detection in fan-out free circuits using minimal single fault test set', *IEEE Trans. Comput.*, 1996, **45**, (6), pp. 763-765
- KAGLE, B.J., MURPHY, J.H., KOOS, L.M., and REEDER, J.R.: 'Multi-fault diagnosis of electronic circuit boards using neural networks'. IJCNN, Washington, 1990, pp. II-197-202

## Hopfield learning rule with high capacity storage of time-correlated patterns

A. Storkey and R. Valabregue

*Indexing term: Hopfield neural networks*

A new local and incremental learning rule is examined for its ability to store patterns from a time series in an attractor neural network. This learning rule has a higher capacity than the Hebb rule, and suffers significantly less capacity loss as the correlation between patterns increases.

**Introduction:** There are two rules regularly used for training Hopfield networks. The most common of these, the Hebb rule, suffers severe degradation when training patterns are correlated. As a result, practitioners have generally reverted to using the pseudo-inverse rule in such circumstances. However the pseudo-inverse method suffers from significant problems. First, it is not incremental: if a new pattern is to be trained, all the old patterns have to be

retrained. Secondly, it is not local: the network cannot naturally be trained in a parallel manner, and so is not easily amenable to high-speed parallel techniques. Lastly, the training method is slow because it involves inverting an  $m \times m$  matrix, where  $m$  is the number of patterns to be stored.

These problems are most significant when the patterns to be trained are a time series and real-time training is needed. The slow speed of the pseudo-inverse, and more importantly its inability to add patterns incrementally, make it of little use for this task. Furthermore, time series usually include significant correlations between readings from adjacent time steps. This makes the Hebb rule unsuitable.

Here, we examine the new learning rule introduced in [1] for its effectiveness with time correlated patterns. This learning rule does not suffer from the disadvantages of the pseudo-inverse: it is both local and incremental. It also has a higher capacity than the Hebb rule. We demonstrate that this new learning rule maintains its high capacity with significant correlations in patterns. This contrasts with the Hebb rule, where the capacity reduces much faster as the correlation increases. We show how this can be accounted for by the relationship between the new rule and the pseudo-inverse.

In this Letter, we look at a model of pattern correlations, which resemble the correlations in patterns which form a time series. Many time series are digitisations of continuous events, digitised both in the time and space domains. For example, video footage consists of frames of digitised video information. Any two frames of such time series are inevitably correlated, the level of correlation depending on the speed of movement, the sampling rate, and how close in time the two frames are to one another.

**The Hopfield network:** The Hopfield network is an attractor neural network which acts as a content addressable memory. The job of the learning rule of a Hopfield network is to find some weight matrix  $w_{ij}$  which stores the required patterns as fixed points of the network.

Locality and incrementality have already been discussed in the introduction. These are both important characteristics of a learning rule. In addition to these, a learning rule has a capacity. This is some measure of how many patterns can be stored in a network of a given size. More specifically, in this Letter we consider the absolute capacity [2] of the network. This is given by the asymptotic ratio of the number of patterns that can be stored without error to the number of neurons, as the network size tends to infinity.

**Different learning rules:** Three learning rules are used in this Letter. The Hebbian learning rule is local and incremental, but has a low absolute capacity of  $n/(2 \ln n)$  where  $n$  is the number of neurons [2]. This capacity decreases significantly if patterns are correlated.

The Pseudo inverse has a capacity of  $n$  [3], but does not have the functionality of the Hebb rule. It is not incremental or local, because it involves the calculation of an inverse.

**The new learning rule:** To overcome the problems of both of these learning methods we introduce the following new learning rule.

**Definition 1 (new learning rule):** The weight matrix  $w_{ij}$  of an attractor neural network is said to follow the new learning rule if it obeys

$$w_{ij}^0 = 0 \quad \forall i, j \quad \text{and} \quad w_{ij}^\nu = w_{ij}^{\nu-1} + \frac{1}{n} \xi_i^\nu \xi_j^\nu - \frac{1}{n} \xi_i^\nu h_{ji}^\nu - \frac{1}{n} h_{ij}^\nu \xi_j^\nu \quad (1)$$

where  $h_{ij}^\mu = \sum_{k=1, k \neq i, j}^n w_{jk}^{\mu-1} \xi_k^\mu$  is a form of local field at neuron  $i$  (the input to the neuron  $i$ ) and  $\xi^\mu$  is the new pattern to be learnt ( $\xi_i^\mu = \pm 1$ ).

This rule is local:  $w_{ij}$  depends only on information available at the two adjacent neurons (the values of  $\xi_i, \xi_j, h_i, h_j$ ). It is clear from the recursive nature of eqn. 1 that it is also incremental. It has an absolute capacity of  $n/\sqrt{2 \ln n}$  [1].

**Capacity:** The measures of absolute capacity given above only hold for independent patterns. Here we consider what happens when patterns are correlated. We are specifically interested in the types of correlations which occur in time series. To model this we form the patterns using the following simple Markov chain: